

Probing carbon nanoparticles in CN_x thin films using Raman spectroscopy

Debdulal Roy,¹ Manish Chhowalla,² Niklas Hellgren,³ T. W. Clyne,¹ and G. A. J. Amaratunga²
¹*Department of Materials Science and Metallurgy, Pembroke Street, University of Cambridge, Cambridge-CB2 3QZ, United Kingdom*

²*Department of Engineering, University of Cambridge, Cambridge-CB2 1PZ, United Kingdom*

³*Frederick Seitz Materials Research Laboratory, University of Illinois at Urbana-Champaign, 104 South Goodwin Avenue, Urbana, Illinois 61801, USA*

(Received 8 March 2004; published 14 July 2004)

Carbon nitride films prepared by magnetron sputtering were studied by multiwavelength Raman spectroscopy. The low/intermediate wavenumber features observed near 400 and 700 cm^{-1} are addressed, and the relaxation of the Raman selection rule due to curvature of the graphene planes in the nanoparticles (similar to carbon nanoions) embedded in CN_x thin films is invoked to explain the possible origin of the near 700 cm^{-1} band. The shift in the G peak center and I_D/I_G ratio are correlated with the observed microstructural changes (published before) in order to understand the effect of nitrogenation and deposition temperature on the structure of the films.

DOI: 10.1103/PhysRevB.70.035406

PACS number(s): 68.65.La, 42.62.Fi, 78.30.Jw, 82.35.Np

I. INTRODUCTION

Since the discovery of diamond-like-carbon film in 1971 by Chabot *et al.*,¹ considerable efforts have been made to improve and tailor the properties of the films using various synthesis techniques.²⁻⁷ A set of carbon-based thin films such as hydrogenated DLC (DLC:H), nitrogen-doped DLC (DLC:N), tetrahedral carbon (ta-C), hydrogenated ta-C, and CN_x films have been produced with aiming to achieve high hardness, manageable stress, and good adhesion. On the other hand C_3N_4 has theoretically been predicted to be a superhard material,⁸ but little has been achieved in synthesizing it in the form of a thin film. Among these carbon films CN_x films exhibit remarkably superior properties for application such as wear resistance coatings.⁵ CN_x films can be synthesized by different techniques including reactive sputtering,⁵ a filtered cathodic vacuum arc (FCVA), plasma-enhanced chemical vapor deposition (PECVD), and electron cyclotron wave resonance (ECWR). CN_x films prepared by various techniques have different structures, and therefore exhibit different properties. For example, films prepared by PECVD contain considerable amounts of H and are less dense,⁷ whereas CN_x films prepared by reactive sputtering contain carbon nanoparticles in a diamondlike-carbon matrix and are hydrogen-free.⁶

Structurally, CN_x films can be considered as a nanocomposite thin film having fullerene-like nanoparticles (soft) in a DLC matrix (hard).⁴ The incorporation of nitrogen in the deposition chamber is believed to promote formation of pentagonal rings in the graphene sheets inducing curvature in the basal plane of graphite and facilitates cross-linking between the planes.^{4,9} Such cross-linked carbon films from N have also been synthesized.^{10,11} Such films have shown the characteristic of being highly elastically deformable. It has been proposed that this is due to underloading most of the strain being accommodated in these curved nanoparticle-like regions. This characteristic leads to a significant improvement in the toughness of the film.⁴ Various characterization techniques such as Raman spectroscopy,^{7,12-16} infrared

spectroscopy,^{7,15} electron energy loss spectroscopy (EELS),¹⁴ x-ray photoelectron spectroscopy (XPS),¹⁶ and nanoindentation¹⁷ have been used to characterize these films. Among these, Raman spectroscopy is one of the most easy-to-use and informative techniques. It is capable of distinguishing different C-C bonding in all kinds of carbon structures, such as diamond, graphite, carbon nanotubes, fullerenes, amorphous carbon, and DLCs. Raman spectroscopy is widely used to characterize DLC films for research as well as for quality control in an industrial production line. Unlike crystalline structures such as graphite and diamond, the Raman selection rule (wave vector $k \approx 0$) is relaxed in amorphous structures. Therefore, a wide band instead of sharp peaks, is observed in the spectrum. Furthermore, Raman scattering from π bonding is more than 50 times stronger than that from σ bonds.¹⁸ Therefore, there are different degrees of resonances of the G (graphitic) and the D (disorder

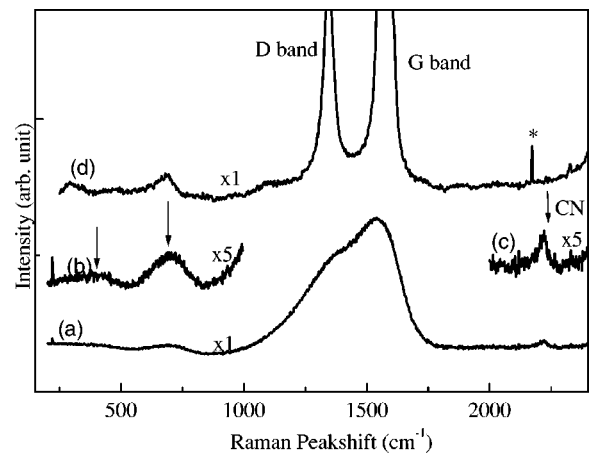


FIG. 1. 514 nm laser Raman spectrum of CN_x and carbon nanoions. (a) Raman spectrum of CN_x ; (b) magnified low/intermediate wave number region of the spectrum of CN_x ; (c) the magnified 2210 cm^{-1} band from the spectrum of CN_x ; (d) the Raman spectrum of carbon nanoions.

TABLE I. List of assignment to the near 700 cm^{-1} peak observed in CN_x films.

Author	Assignment	Reference Number
Kumar <i>et al.</i>	Out of plane sp^3 -type C–C bonding	21
Chowdhury <i>et al.</i>	Nitrogenated carbon	20
Rodil <i>et al.</i>	In-plane-rotation of six-fold rings in graphitic layers	15
Li <i>et al.</i>	Disorder-induced Raman scattering (DIRS) in glassy carbon	13
Tamor <i>et al.</i>	Raman inactive acoustic and out-of-plane optical vibrational modes of graphite	18
Roy <i>et al.</i>	Out of plane transverse optic phonon near the M point zone boundary induced by curvature of graphene planes	22

induced) bands,¹⁹ which prohibit direct estimation of the % sp^3 and % sp^2 bonding.

II. EXPERIMENTAL DETAILS

In this work, the CN_x films were prepared by reactive dc magnetron sputtering in mixed Ar/ N_2 discharges using a pyrolytic graphite disk as the target.⁴ The details of the deposition process are published elsewhere.⁵ All the films were deposited at a constant pressure of 3 mTorr and with a N_2 concentration varying from 0% to 100%. Substrate temperatures were 100 °C, 350 °C, and 550 °C, and it was monitored by a calibrated thermocouple in the substrate holder. Raman measurements were performed using Renishaw Raman microscope with different excitation wavelength including 325, 488, 514, 633, and 785 nm. Care was taken to avoid damage due to laser heating during the measurements. The spectral resolutions were between 2–4 cm^{-1} . Chemical composition of the films was analyzed by x-ray photoelectron spectroscopy (XPS) using VG Microlab 310F instrument.

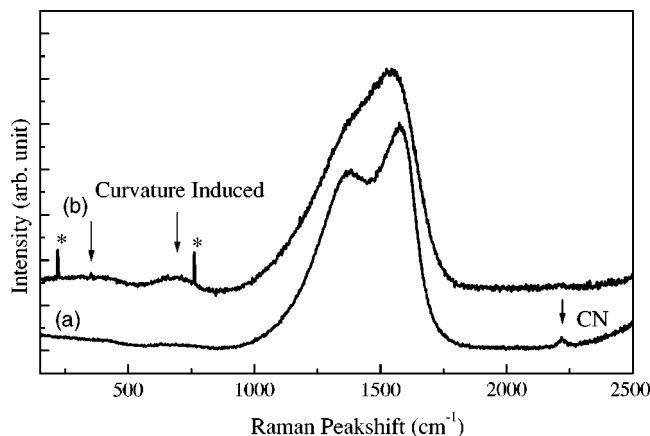


FIG. 2. Normalized Raman spectra of CN_x films with a 488 nm laser: (a) a Raman spectrum showing a relatively intense 2200 cm^{-1} from $\text{C}\equiv\text{N}$ vibration but a very weak 400 and 700 cm^{-1} band; (b) the Raman spectrum showing relatively intense 400 and 700 cm^{-1} bands but a significantly weak 2200 cm^{-1} band.

III. RESULTS AND DISCUSSIONS

Four characteristic features are observed in a Raman spectrum of a CN_x film: two low/intermediate wave number bands near 400 cm^{-1} and near 700 cm^{-1} , broad and an overlapped D and G band similar to that of DLC in the region of 1000–2000 cm^{-1} and a weak feature near 2210 cm^{-1} [Figs. 1(a)–1(c)]. The low/intermediate bands and the 2210 cm^{-1} band from Fig. 1(a) are shown five times magnified in Figs. 1(b) and 1(c), respectively. Similar spectra have also been reported by other authors.^{12,14–16} The assignment of the band near 700 cm^{-1} is controversial. Some of the assignments by different authors are listed in Table I. Often it is associated to sp^3 -carbon-related vibration.^{20,21} Tamor *et al.* observed the band only from nonhydrogenated amorphous carbon films.¹⁸ However, this weak intermediate wave number feature has also been observed from nitrogenated carbon films with or without hydrogen. Li *et al.* reported Raman bands centered around ~ 430 and 800 cm^{-1} from glassy carbon and assigned them to disorder-induced Raman scattering (DIRS).¹³ In this work, two distinct bands were observed always together near 400 and 700 cm^{-1} : the ~ 700 cm^{-1} band being more intense than the ~ 400 cm^{-1} band. Similar bands also appeared in the Raman spectrum acquired from carbon nano-onions [Fig. 1(d)]. The details of the assignment of the bands from carbon nano-onions has been published elsewhere.²² Relaxation of the Raman selection rule due to curvature in graphene planes appears to induce Raman scattering away from the Γ point. The bands that appeared near 400 cm^{-1} and near 700 cm^{-1} from carbon nano-onions have been assigned to the trans-

TABLE II. Raman peak centers of the near 700 cm^{-1} band and the near 400 cm^{-1} band measured with lasers of different wavelength.

Laser wavelength	Center of the ~ 700 cm^{-1} band	Center of the ~ 400 cm^{-1} band
488 nm	699 cm^{-1}	365 cm^{-1}
514 nm	722 cm^{-1}	361 cm^{-1}
785 nm	741 cm^{-1}	391 cm^{-1}

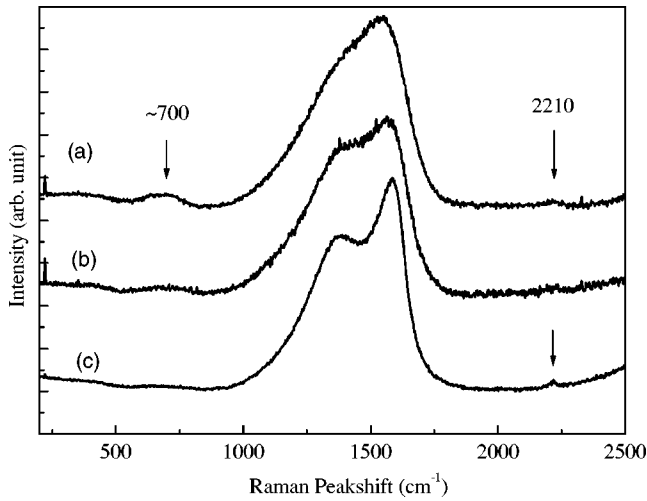


FIG. 3. Raman spectra with 488 nm laser of CN_x films deposited at a different temperature with 100% N₂: (a) Deposited at 100 °C temperature and contain 26% nitrogen (b) deposited at 350 °C and contain 20% nitrogen (c) deposited at 550 °C and contain 17% nitrogen.

verse optic and transverse acoustic vibrations at the M point.²³ It is well known that there are curved graphene planes embedded in an amorphous matrix in CN_x films.^{5,9} These embedded curved graphene planes can exhibit characteristics similar to carbon onions,²⁴ or these can be bowl-shaped;⁴ therefore, the two low/intermediate wave number bands similar to those from carbon nano-onions are also expected to appear from CN_x films. Indeed their intensities depend upon the concentration of these nano-particle/curved graphene planes in the film. These two Raman bands were fitted with two Gaussian functions and the centers of these peaks are listed in Table II at different laser energies for a film deposited at 350 °C. From the systematic variation of the ~700 cm⁻¹ peak it is clear that there is significant dispersion of that band. It is possible that there is also some

contribution from the maxima of the PDOS to the intensity of the two bands. However, if it originates only from the maxima of PDOS, it is not expected to exhibit dispersion. No obvious trend could be observed for the near 400 cm⁻¹ band. It is noticed that the bands from CN_x films are broader than those from carbon onions. This is presumably due to large distribution of curvature of the graphene planes in the CN_x films.

The peak that appears near 2200 cm⁻¹ is assigned to C≡N bonding.¹⁵ N₂ plays a role in the formation of the curved graphene planes in these films, however, the low/intermediate bands are not related to vibrations of C≡N bonding. This is confirmed in Fig. 2 where two Raman spectra from two different films are shown. A relatively strong 2200 cm⁻¹ band can be seen in Fig. 2(a) with very weak low/intermediate wave number bands, whereas in Fig. 2(b) a relatively weak 2200 cm⁻¹ band and strong low/intermediate wave number bands can be observed: it is clear that these two features are not due to the same structural characteristic. From the above analysis we propose that the low/intermediate wave number Raman bands from CN_x films appear due to curvature in the graphene planes, and their intensities are not related to C≡N bonding. However, nitrogen can form different bonding with carbon and it is difficult to correlate the intensities of the low/intermediate bands with any other particular type of nitrogen-carbon bonding.

Significant variations were observed in the *D* and *G* bands of the CN_x films deposited at different temperatures. Films grown at 100 °C, 350 °C and 550 °C are shown in Fig. 3. *D* and *G* bands dominate in the Raman spectrum of any amorphous carbon.¹⁸ The *G* band that appears between 1500–1600 cm⁻¹ is due to the *E*_{2g} vibrational mode of a graphitic structure. The band that appears near 1350 cm⁻¹ is described as a *D* band: a disorder-induced Raman band. Double resonance phenomenon is invoked to explain the origin of the *D* band in graphitic structures.^{25,26} The *D* band is absent in highly perfect graphite and it appears in all other defected graphitic structures.¹⁹ The ratio of *D* and *G* band

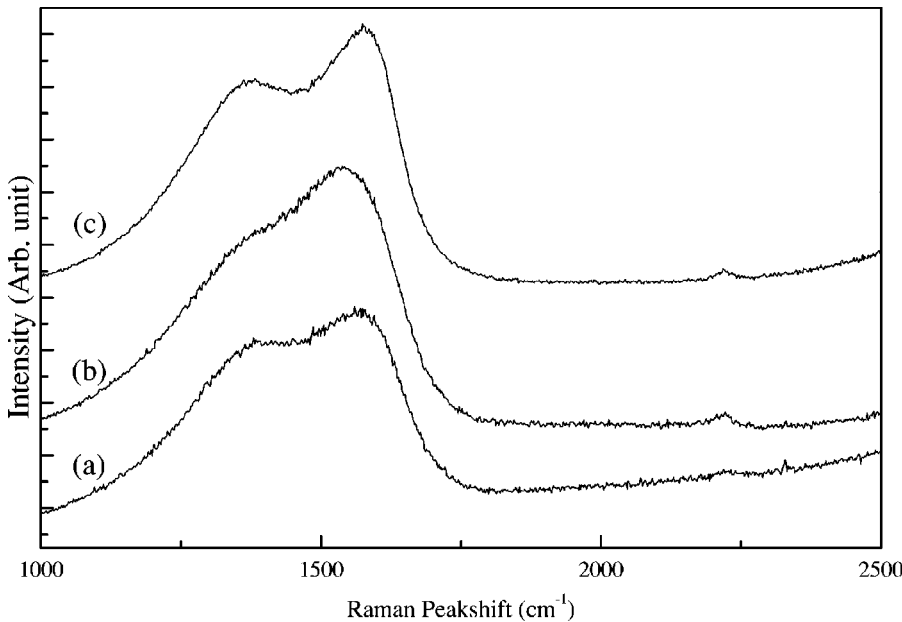


FIG. 4. Raman spectra with 488 nm laser of CN_x films grown at 350 °C having (a) 1% nitrogen, (b) 12% nitrogen, (c) 20% nitrogen.

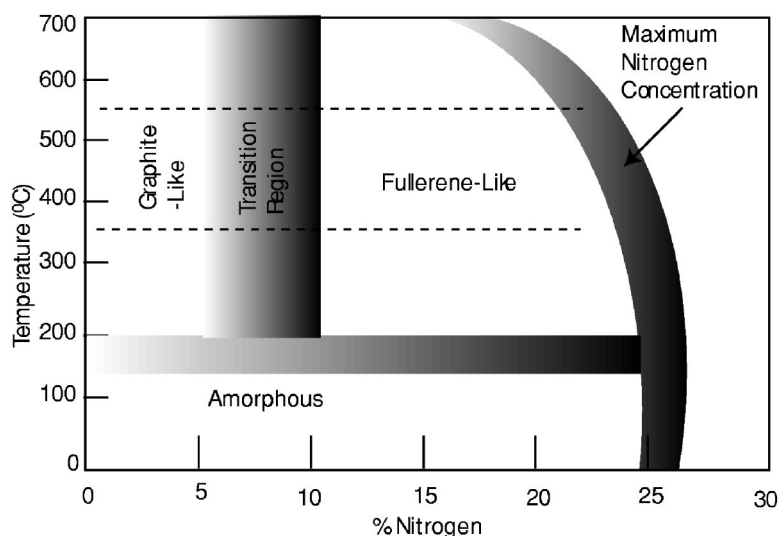


FIG. 5. Schematic phase of CN_x films deposited by reactive magnetron sputtering after Hellgren *et al.* (Ref. 4).

intensities (I_D/I_G) is often used as a measure of the size of graphitic domains in DLC films.^{19,27} For example, ta-C films that have a $>80\%$ sp^3 component shows a very weak D band. The G band was fitted with a Breit-Wigner-Fano (BWF) function and the D peak was fitted with a Lorentzian function to estimate the peak parameters. This fitting method has been widely used for a quantitative analysis of the D and G peak intensities for a variety of carbon structures.^{27–29} For various resonance mechanisms, the D peak is consistently Lorentzian.²⁷ The asymmetry of BWF lineshape arises from coupling of discrete mode to a continuum and the degree of asymmetry depends on the value of the coupling coefficient. For example, for a continuous crystal, the coupling coefficient becomes zero and the curve takes a symmetric Lorentzian lineshape. On the other hand, for a disordered system, the lineshape becomes very asymmetric (refer to Ref. 27 for details). CN_x films falls somewhere between a completely disordered system and continuum,⁶ therefore a BWF lineshape was used for fitting the G peak.

The temperature effect on the Raman spectra are shown in Fig. 3. It can be seen that the D band that appears as a shoulder in Fig. 3(a) separates out in Fig. 3(c). As the deposition temperature increases, long range ordering in the graphitic structures increases and the D peak becomes more prominent. Effect of nitrogenation in the films grown at $350^\circ C$ is shown in Fig. 4. Films having low %N [e.g., 1% in Fig. 4(a)] show a broad G peak and a broad D peak as a shoulder. However, the D peak becomes less prominent as the %N increases to 12%. Nitrogen is expected to increase the sp^3 content in the films, which is reflected in a reduction in D peak intensity.^{12,30} With a further increase of the nitrogen content to 20%, the D peak separates out from the overlapped spectrum. The peak near 2200 cm^{-1} is due to the $-C\equiv N$ vibration, as discussed above.

As described by Hellgren *et al.*⁴ by a phase diagram there are three distinct regions where three different microstructures are formed corresponding to different nitrogen concentrations and temperatures. The phase diagram is shown in Fig. 5. For example, below $150^\circ C$ and less than 25% N, it forms an amorphous structure, above $200^\circ C$ and less than 5% N, the structure is graphitelike, and between

$200^\circ C$ – $600^\circ C$ and 10%–20% N, it forms a fullerene-like structure. It is known that the G peak center and the I_D/I_G ratio vary with the structure of DLC films.²⁷ The variation of the G peak center and I_D/I_G against %N in the films deposited at $350^\circ C$ and $550^\circ C$ are shown in Figs. 6 and 7, respectively. It is seen that both the G peak position and I_D/I_G ratio decreases sharply near 5% N, where the transition in the structural change is expected, before stabilizing. A similar trend is observed for the films grown at $550^\circ C$. Therefore, it is clear from the trends that the G peak center and I_D/I_G ratio decrease in the region ($>5\%$ N) where a fullerene-like structure is formed. A downshift of the G peak center is normally observed with an increase in the nitrogen content in CN_x films prepared by magnetron sputtering.¹² Nitrogen incorporation in the films enhances sp^3 characteristic in the carbon bonds due to crystallinity of the graphene planes, due to the N-induced formation of pentagonal rings. Consequently, the

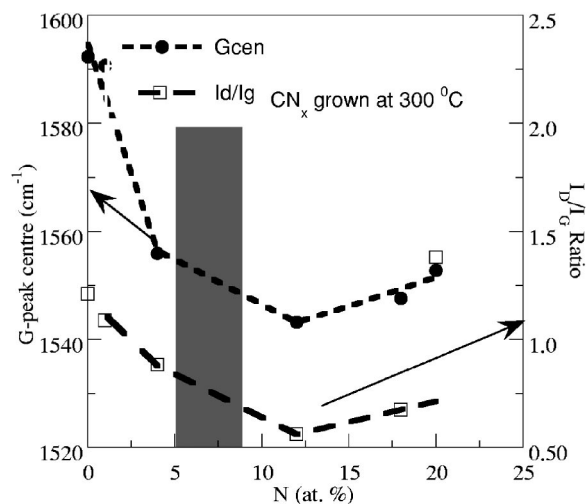


FIG. 6. Shift of the G peak center and variation of the I_D/I_G ratio with %N for the CN_x films deposited at $350^\circ C$. Measurements were performed using a 514 nm laser. Broken lines are drawn to guide the eyes. A transition region near 5% N is shown in shade.

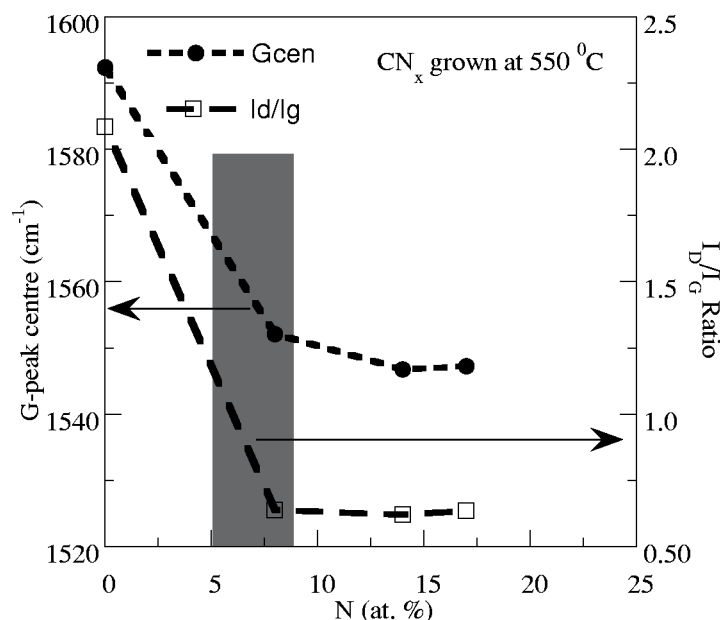


FIG. 7. Shift of the G peak center and variation of the I_D/I_G ratio with %N for the CN_x films deposited at 350 °C. Measurements were performed using a 514 nm laser. Broken lines are drawn to guide the eyes. A transition region near 5% N is shown in shade.

G peak center is shifted downward.¹² This is also reflected in the decrease of the I_D/I_G ratio. The G peak center of the film deposited at 350 °C with no nitrogen is 1590 cm^{-1} (Fig. 6), which is a characteristic of a graphitelike amorphous structure, and it shifts down to 1550 cm^{-1} as the nitrogen concentration increases to 10%. However, Rodill *et al.*¹⁵ observed opposite trends (Fig. 4 in Ref. 15) on the shift of the G peak center and variation of the I_D/I_G ratio with increasing %N. It is exactly the opposite effect of nitrogen incorporation in these two types of films. The films prepared by ECWR without any nitrogen contain as high as 80% sp^3 carbon, and, when nitrogen is incorporated, it decreases sp^3 content and shifts the G peak position upward (e.g., from 1535 to 1570 cm^{-1} in Ref. 15). Therefore, the structure of CN_x films prepared by different techniques appears to vary differently with nitrogen incorporation.

IV. CONCLUSIONS

In summary, we have discussed the characteristic features of the visible Raman spectrum of CN_x film that can display a similar fullerene-like structure. The low/intermediate wave number bands observed from CN_x films were correlated with those observed from carbon nano-onions. Considering the microstructure of the films and characteristic Raman spectrum of carbon onions, it is suggested that the curvature of the graphene planes observed in CN_x films may induce these new Raman bands. Scattering from the transverse optic phonon near the M point is a possible origin of the near 700 cm^{-1} band. However, there may also be some intensity contribution from the maxima of the phonon density of states. The effect of nitrogen incorporation and temperature on the Raman spectra of CN_x films is demonstrated. The variation of the G peak position and I_D/I_G ratio with %N is explained in the context of a structural change.

¹S. Aisenberg and R. Chabot, *J. Appl. Phys.* **42**, 2953 (1971).

²M. Chhowalla, Y. Yin, G. A. J. Amaratunga, and D. R. McKenzie, *Appl. Phys. Lett.* **69**, 2344 (1996).

³X. L. Peng and T. W. Clyne, *Thin Solid Films* **312**, 207 (1998).

⁴N. Hellgren, M. P. Johansson, E. Broitman, P. Sandstrom, L. Hultman, and J. E. Sundgren, *Phys. Rev. B* **59**, 5162 (1999).

⁵N. Hellgren, M. P. Johansson, E. Broitman, P. Sandstrom, L. Hultman, and J. E. Sundgren, *Thin Solid Films* **382**, 146 (2001).

⁶N. Hellgren, M. P. Johansson, B. Hjorvarsson, E. Broitman, M. Ostblom, B. Liedberg, L. Hultman, and J. E. Sundgren, *J. Vac. Sci. Technol. A* **18**, 2349 (2000).

⁷S. R. P. Silva, J. Robertson, G. A. J. Amaratunga, B. Rafferty, L. M. Brown, J. Schwan, D. F. Franceschini, and G. Mariotto, *J.*

Appl. Phys. **81**, 2626 (1997).

⁸A. Y. Liu and M. L. Cohen, *Science* **245**, 841 (1989).

⁹L. Hultman, S. Stafström, Z. Czizgány, J. Neidhardt, N. Hellgren, I. F. Brunell, K. Suenaga, and C. Colliex, *Phys. Rev. Lett.* **87**, 225503 (2001).

¹⁰G. A. J. Amaratunga, M. Chhowalla, C. J. Kiely, I. Alexandrou, R. Aharonov, and M. Devenish, *Nature (London)* **383**, 321 (1996).

¹¹I. Alexandrou, H. J. Scheibe, C. J. Kiely, A. J. Papworth, G. A. J. Amaratunga, and B. Schultrich, *Phys. Rev. B* **60**, 10903 (1999).

¹²M. Neuhaeuser, H. Hilgers, H. Joeris, R. White, and J. Windeln, *Diam. Relativ. Mater.* **9**, 1500 (2000).

¹³F. Li and J. S. Lannin, *Appl. Phys. Lett.* **61**, 2116 (1992).

- ¹⁴M. Y. Chen, D. L. X. Lin, V. P. Dravid, Y. Chung, M. Wong, and W. D. Sproul, *J. Vac. Sci. Technol. A* **11**, 521 (1993).
- ¹⁵S. E. Rodil, A. C. Ferrari, J. Robertson, and W. I. Milne, *J. Appl. Phys.* **89**, 5425 (2001).
- ¹⁶F. Parmigiani, E. Kay, and H. Seki, *J. Appl. Phys.* **64**, 3031 (1988).
- ¹⁷H. Sjöström, L. Hultman, J.-E. Sundgren, S. V. Hainsworth, T. F. Page, and G. S. A. M. Theunissen, *J. Vac. Sci. Technol. A* **14**, 56 (1996).
- ¹⁸M. A. Tamor and W. C. Vassel, *J. Appl. Phys.* **76**, 3823 (1994).
- ¹⁹F. Tuinstra and J. L. Koenig, *J. Chem. Phys.* **53**, 1126 (1970).
- ²⁰A. K. M. S. Chowdhury, D. C. Cameron, and M. S. J. Hashmi, *Thin Solid Films* **332**, 62 (1998).
- ²¹S. Kumar and T. L. Tansley, *Thin Solid Films* **256**, 44 (1995).
- ²²D. Roy, M. Chhowalla, H. Wang, N. Sano, I. Alexandrou, T. W. Clyne, and G. A. J. Amaratunga, *Chem. Phys. Lett.* **373**, 52 (2003).
- ²³R. Al-Jishi and G. Dresselhaus, *Phys. Rev. B* **26**, 4514 (1982).
- ²⁴E. D. Obraztsova, M. Fujii, S. Hayashi, V. L. Kuzentsov, V. Butenko, and A. L. Chuvilin, *Carbon* **36**, 821 (1998).
- ²⁵C. Thomsen and S. Reich, *Phys. Rev. Lett.* **85**, 5214 (2000).
- ²⁶R. Saito, A. Jorio, A. G. Filho, G. Dresselhaus, M. S. Dresselhaus, and M. A. Pimenta, *Phys. Rev. Lett.* **88**, 027401 (2002).
- ²⁷A. C. Ferrari and J. Robertson, *Phys. Rev. B* **61**, 14095 (2000).
- ²⁸D. G. McCulloch and S. Prawer, *J. Appl. Phys.* **78**, 3040 (1995).
- ²⁹D. G. McCulloch, S. Prawer, and A. Hoffman, *Phys. Rev. B* **50**, 5905 (1994).
- ³⁰C. J. Torng, J. M. Sivertsen, J. H. Judy, and C. Chang, *J. Mater. Res.* **5**, 2490 (1990).